PARTICLE PRODUCTION IN HIGH-ENERGY HEAVY-ION COLLISIONS

XIN-NIAN WANG
Nuclear Science Division, Lawrence Berkeley National Laboratory, Berkeley, California, 94720
Department of Physics, Shandong University, Jinan, P.R.China, 250100

Particle production mechanisms in high-energy heavy-ion collisions are reviewed in connection with recent experimental data from RHIC. Implications on mini-jet production, parton saturation and jet quenching are discussed.

1 Introduction

Quark-gluon plasma (QGP) is expected to form in high-energy heavy-ion collisions. Though some proposed signals can provide more direct measurements of the initial parton density, many must reply on information inferred indirectly from the measurement of final hadron spectra. Therefore, both global observables such as the rapidity density of hadron multiplicity and high p_T hadron spectra can provide important links of a puzzle that can eventually lead one to a more complete picture of the dynamics of heavy-ion collisions and formation of QGP.

Mini-jet production in a two-component model has long been proposed to explain the energy dependence of total cross section [1,2] and particle production [3,4] in high-energy hadron collisions. It has also been proposed [6,5] and incorporated in the HIJING model [7,8] to describe initial parton production in high-energy heavy-ion collisions. In this model, parton production from semi-hard processes becomes quite significant, giving rise to the high initial parton density in high-energy heavy-ion collisions. However, there are still quite large uncertainties due to the lack of knowledge of the initial parton distributions in nuclei and the final state interaction of produced partons. Therefore, the study of energy and centrality dependence of central rapidity density [9] can provide important constraints on models of initial entropy production and shed lights on the initial parton distributions in nuclei. For example, the available RHIC experimental data [10,11,12,13,14] can already rule out the simple two-component model without nuclear modification of the parton distributions in nuclei [9]. However, further studies are needed to constrain the unknown nuclear shadowing of the gluon distribution in nuclei and to further distinguish the conventional parton production mechanism from other novel physics such as parton saturation [15,16].

Among the produced particle, a few have very high transverse momentum. They are related to high-energy jet production which is a very useful tool to study the properties of dense matter formed in high-energy heavy-ion collisions. Because large p_T partons are produced very early in heavy-ion collisions and their production rates can be calibrated in pp and pA collisions at the same energy, they are ideal probes of the dense matter that is formed in the same reaction. What probes the dense medium is the scattering induced energy loss suffered by an energetic parton as it propagates through the matter. The parton energy loss is directly related to the parton density of the medium. These are the main topics of this talk.

2 Two-component model

In the two-component model, the soft and hard processes are separated by a cut-off scale p_0. While the cross section of soft interaction $\sigma_{\rm soft}$ is considered nonperturbative and thus noncalculable, the jet production cross section $\sigma_{\rm jet}$ is assumed to be given by perturbative QCD (pQCD) for transverse momentum transfer $p_T > p_0$. The two parameters, $\sigma_{\rm soft}$ and p_0, are determined phenomenologically by fitting the experimental data of total $p+p(\bar{p})$ cross sections within the two-component model [1,2,3,4,7,8]. The cut-off scale p_0, separating nonperturbative and pQCD components, could in principle depend on both energy and nuclear size. Using the Gluck-Reya-Vogt (GRV) parameterization [17] of parton distributions and following the same procedure as in the original HIJING [7], one finds that the cut-off scale must have a weak energy dependence,

$$p_0(\sqrt{s}) = 3.91 - 3.34\log(\log\sqrt{s}) + 0.98\log^2(\log\sqrt{s}) + 0.23\log^3(\log\sqrt{s}), \quad (1)$$

in order to fit the experimental data, because of the rapid increase of gluon distribution at small x. Shown in Fig. 1 is the calculated central rapidity density,

$$\frac{dN_{\rm ch}}{d\eta} = \langle n\rangle_{\rm s} + \langle n\rangle_{\rm h}\frac{\sigma_{\rm jet}(s)}{\sigma_{\rm in}(s)}, \quad (2)$$

for $p+p(\bar{p})$ collisions as a function of energy $\sqrt{s}$, where $\langle n\rangle_{\rm s} = 1.6$ and $\langle n\rangle_{\rm h} = 2.2$ represent particle production from soft interaction and jet hadronization, respectively. The jet cross section is the lowest order pQCD result with a K-factor of 2 and GRV parton distributions.

To extrapolate the two-component model to nuclear collisions, one assumes that multiple mini-jet production is incoherent and thus is proportional

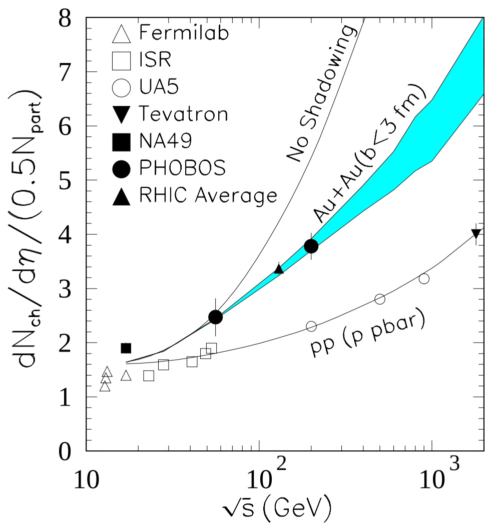

Figure 1. Charged particle rapidity density *per participating nucleon pair* versus the c.m. energy. The RHIC data[10,11] (filled circle and up-triangle) for the 6% most central Au+Au are compared to pp and $p\bar{p}$ data (open symbols) [18,19,20] and the NA49 $Pb+Pb$(central 5%) data [21] (filled square). The two-component mini-jet model with and without shadowing is also shown. The shaded area for central $Au+Au$ collisions corresponds to the range of gluon shadowing parameter $s_g = 0.24$–0.28 [Eq. (4)].

to the number of binary collisions $N_{\rm binary}$. The soft interaction is however coherent and proportional to the number of participant nucleons $N_{\rm part}$ according to the wounded nucleon model [22]. One important nuclear effect we have to consider in the two-component model is the nuclear shadowing of parton distributions in nuclei at small x. Such a nuclear shadowing effect in jet production can be taken into account by assuming modified parton distributions in nuclei,

$$f_a^A(x,Q^2) = AR_a^A(x,Q^2)f_a^N(x,Q^2). \tag{3}$$

Using the experimental data from DIS off nuclear targets and unmodified DGLAP evolution equations, one can parameterize $R_a^A(x,Q^2)$ for different partons and nuclei. Recent new data however indicate that the simple parameterization for nuclear shadowing used in HIJING is too strong [23] for heavy nuclei. Instead one has to use the following new parameterization,

$$R_a^A(x) = 1.0 + 1.19\log^{1/6}\!A\;(x^3 - 1.2x^2 + 0.21x)$$

$$- \, s_a \, (A^{1/3} - 1)^{0.6} (1 - 3.5\sqrt{x}) \exp(-x^2/0.01) \qquad (4)$$

with $s_q = 0.1$ for all quark distributions and $s_g = 0.24$–0.28 for gluon. Assuming no final state effects on multiplicity from jet hadronization, the rapidity density of hadron multiplicity in heavy-ion collisions as shown in Fig. 1 is,

$$\frac{dN_{ch}}{d\eta} = \frac{1}{2}\langle N_{\rm part}\rangle \langle n\rangle_s + \langle n\rangle_h \langle N_{\rm binary}\rangle \frac{\sigma_{\rm jet}^{AA}(s)}{\sigma_{\rm in}}, \qquad (5)$$

where $\sigma_{\rm jet}^{AA}(s)$ is the averaged inclusive jet cross section per NN in AA collisions including parton shadowing effect. The average number of participant nucleons and number of binary collisions for given impact-parameters can be estimated using HIJING Monte Carlo simulation. It is clear that one has to consider parton shadowing in jet production in heavy-ion collisions.

3 Parton Saturation

Similar results of multiplicity in heavy-ion collisions are also predicted by other models [24,25], in particular the initial-state parton saturation model [15,16]. It is based on the nonlinear Yang-Mills field dynamics [5,26] assuming that nonlinear gluon interaction below a saturation scale $Q_s^2 \sim \alpha_s \, xG_A(x,Q_s^2)/\pi R_A^2$ leads to a classical behavior of the gluonic field inside a large nucleus, where $G_A(x,Q_s^2)$ is the gluon distribution at $x = 2Q_s/\sqrt{s}$. Assuming particle production in high-energy heavy-ion collisions is dominated by gluon production from the classical gluon field, one has a simple form [16] for the charged hadron rapidity density at $\eta = 0$,

$$\frac{2}{\langle N_{\rm part}\rangle}\frac{dN_{ch}}{d\eta} = c\left(\frac{s}{s_0}\right)^{\lambda/2}\left[\log\left(\frac{Q_{0s}^2}{\Lambda_{\rm QCD}^2}\right) + \frac{\lambda}{2}\log\left(\frac{s}{s_0}\right)\right], \qquad (6)$$

with $c \approx 0.82$ [15]. This is shown in Fig. 4 as solid lines as compared to the two-component model (shaded area). Here, $\Lambda_{\rm QCD} = 0.2$ GeV, $\lambda = 0.25$ and the centrality dependence of the saturation scale Q_{0s}^2 at $\sqrt{s_0} = 130$ GeV is taken from Ref. [15]. The two-component model has an impact-parameter dependent parton shadowing.

Comparing the two model results in Fig. 2, one notices that the saturation and two-component model agree with each other in most regions of centrality except very peripheral and very central collisions. In central collisions, results of saturation model tend to be flatter than the two-component model. In this region, there are still strong fluctuations in parton production in the two-component model through the fluctuation of $N_{\rm binary}$ while $N_{\rm part}$ is limited by its maximum value of $2A$. That is why $dN_{ch}/d\eta/\langle N_{\rm part}\rangle$ continues to

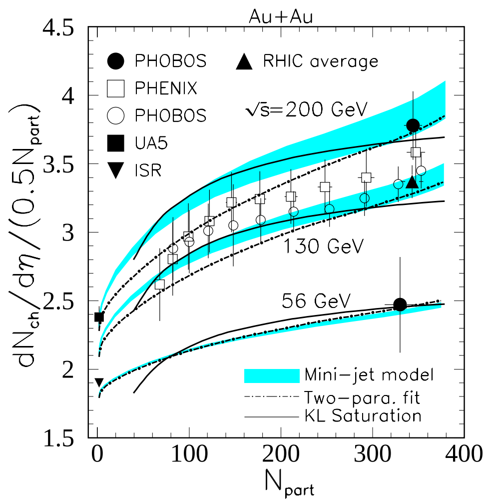

Figure 2. The charged hadron central rapidity density per participant nucleon pair as a function of the averaged number of participants from the two-component model (shaded lines), two-parameter fit [23] (dot-dashed lines) and parton saturation model [16] as compared to experimental data [10,12,18,19].

increase with $\langle N_{\rm part}\rangle$ in the central region. Such a fluctuation is not currently taken into account in the saturation model calculation. More accurate measurements with small errors (less than 5%) will help to distinguish these two different behaviors. For peripheral collisions, saturation model results fall off more rapidly than the mini-jet results. However, the experimental errors are very big in this region because of large uncertainties related to the determination of the number of participants. Therefore, it will be very useful to have light-ion collisions at the same energy to map out the nuclear dependence of the hadron multiplicity in this region. An alternative is to study the ratios of hadron multiplicity of heavy-ion collisions at two different energies as a function of centrality [23]. In this case, the errors associated with the determination of centrality will mostly cancel.

It is interesting to point out that in the saturation model that assumes a particle production mechanism dominated by coherent mini-jet production below the saturation scale Q_s, the value of Q_s determined in Ref.[15,16] is much smaller than the cut-off p_0 in the two-component model constrained by the $p+p(\bar{p})$ data. As demonstrated in this paper, the number of mini-jet production below such scale is still very large and should contribute to the final hadron multiplicity.

4 Parton energy loss

Among the bulk of produced hadrons in heavy-ion collisions, there are also high p_T hadrons produced in events with hard processes. In principle, jet quenching effect could also lead to increased total hadron multiplicity [27] due to the soft gluons from the bremsstrahlung. However, a recent study [28] of parton energy loss in a thermal environment found that the effective energy loss is significantly reduced for less energetic partons due to detailed balance by thermal absorption. Thus, only large energy jets lose significant energy via gluon bremsstrahlung. Since the production rates of these large energy jets are very small at the RHIC energy, their contributions to the total hadron multiplicity via jet quenching should also be small. Similarly we also assume that parton thermalization during the early stage contributes little to the final hadron multiplicity.

Theoretical studies of the parton energy loss in hot medium date back to the first attempt by Bjorken [29] to calculate elastic energy loss of a parton via elastic scattering in the hot medium. A simple estimate can be given by the thermal averaged energy transfer $\nu_{\rm el} \approx q_\perp^2/2\omega$ of the jet parton to a thermal parton with energy ω, $q_\perp$ being the transverse momentum transfer of the elastic scattering. The resultant elastic energy loss [8]

$$\frac{dE_{\rm el}}{dx} = C_2 \frac{3\pi\alpha_{\rm s}^2}{2} T^2 \ln\left(\frac{3ET}{2\mu^2}\right) \tag{7}$$

is sensitive to the temperature of the thermal medium but is in general small compared to radiative energy loss. Here, μ is the Debye screening mass and C_2 is the Casimir of the propagating parton in its fundamental presentation. The elastic energy loss can also be calculated within finite temperature QCD [30] with a similar result, but with a more careful and consistent treatment of screening effect.

Though there had been estimates of the radiative parton energy loss using the uncertainty principle [31], a first theoretical study of QCD radiative parton energy loss incorporating Landau-Pomeranchuk-Migdal interference effect [32] is by Gyulassy and myself [33] where multiple parton scattering is modeled by a screened Coulomb potential model. Baier *et al.* (BDMPS) [34] later considered the effect of gluon rescattering which turned out to be very important for gluon radiation induced by multiple scattering in a dense medium. These two studies have ushered in many recent works on the subject, including a path integral approach to the problem [35] and opacity expansion framework [36,37] which is more suitable for multiple parton scattering in a thin plasma. The radiative parton energy loss to the leading order of the opacity $\bar{n} = L/\lambda$ in the thin plasma of size L is estimated as [36,28]

$$\frac{dE_{\rm rad}}{dx} \approx C_2 \frac{\alpha_{\rm s}\mu^2}{4} \frac{L}{\lambda} \ln\left(\frac{2E}{\mu^2 L}\right), \tag{8}$$

where λ is the gluon's mean-free-path in the medium. The unique L dependence of the parton energy loss is a consequence of the non-Abelian LMP interference effect in a QCD medium. It is also shown in a recent study [28] that thermal absorption and stimulated emission in a thermal environment can be neglected for high energy partons ($E \gg \mu$) while they are important for intermediate energy partons.

Using this latest result one can estimate the total energy loss for a parton with initial energy $E = 40$ GeV to be about $\Delta E \approx 10$ GeV after it propagates a distance of $L = 6$ fm in a medium with $\mu = 0.5$ GeV and $\lambda = 1$ fm. For an expanding system, the total energy loss is reduced by a factor of $2\tau_0/L$ from the static value [38,39]. Assuming that most of this energy loss is carried by gluons outside the jet cone [40], measuring the energy loss would require the experimental resolution δE to be much smaller than the total energy loss ΔE. With the measured total multiplicity density $dN/d\eta \approx 900$ [10] and energy density $dE_T/d\eta \approx 500$ GeV [41] in central $Au + Au$ collisions at $\sqrt{s} = 130$ GeV, one can estimate that the average total background energy within the jet cone ($\delta\eta = 1$ and $\delta\phi = 1$) is about $\Sigma E_T \approx 80$ GeV with a fluctuation of $\delta E_T \approx 10$ GeV. It is therefore very difficult, if not impossible, to determine the energy of a jet on a event-by-event base [42]. Since high p_T hadrons in hadron and nuclear collisions come from fragmentation of high E_T jets, energy loss naturally leads to suppression of high p_T hadron spectra. Miklos Gyulassy and I then proposed [27] that one has to reply on measuring the suppression of high p_T hadrons to study parton energy loss in heavy-ion collisions. Since inclusive hadron spectra is a convolution of jet production cross section and the jet fragmentation function in pQCD, the suppression of inclusive high p_T hadron spectra is a direct consequence of the medium modification of the jet fragmentation function induced by parton energy loss. Assuming that jet fragmentation function is the same for the final leading parton with a reduced energy, the modified fragmentation function can be assumed as [43]

$$\widetilde{D}(z) \approx \frac{1}{1 - \Delta E/E} D\left(\frac{z}{1 - \Delta E/E}\right). \tag{9}$$

Therefore, in this effective model the measured modification of fragmentation function can be directly related to the parton energy loss.

5 Modified fragmentation functions

Since a jet parton is always produced via a hard process involving a large momentum scale, it should also have final state radiation with and without rescattering leading to the DGLAP evolution equation of fragmentation functions. Such final state radiation effectively acts as a self-quenching mechanism softening the leading parton momentum distribution. This process is quite similar to the induced gluon radiation and the two should have strong interference effect [36,37]. It is therefore natural to study jet quenching and modified fragmentation function in the framework of modified DGLAP evolution equations in a medium [44].

The simplest case for jet quenching is deeply inelastic scattering of an electron off a nucleus target where the virtual photon knocks one quark out of a nucleon inside a nucleus. The quark then will have to propagate through the rest of the nucleus and possibly scatter again with other nucleons with induced gluon radiation. The induced gluon radiation reduces the quark's energy before it fragments into hadrons with a modified fragmentation function. One can study the nuclear modification of the fragmentation function by comparing it with the same measurement in DIS with a nucleon target.

In an infinite momentum frame, where the photon carries momentum $q = [-x_B p^+, q^-, \vec{0}_\perp]$ and the momentum of the target per nucleon is $p = [p^+, 0, \vec{0}_\perp]$ with the Bjorken variable defined as $x_B = Q^2/2q^-p^+$, one can calculate the modified fragmentation function. Because of the LPM interference effect, the formation time of the gluon radiation due to the LPM interference requires the radiated gluon to have a minimum transverse momentum $\ell_T^2 \sim Q^2/MR_A \sim Q^2/A^{1/3}$. The nuclear corrections to the fragmentation function due to double parton scattering will then be in the order of $\alpha_s A^{1/3}/\ell_T^2 \sim \alpha_s A^{2/3}/Q^2$, which depends quadratically on the nuclear size. For large values of A and Q^2, these corrections are leading and yet the requirement $\ell_T^2 \ll Q^2$ for the logarithmic approximation in deriving the modified fragmentation function is still valid.

Shown in Fig. 3 are the calculated nuclear modification factor of the fragmentation function for ^{14}N and ^{84}Kr targets as compared to the recent HERMES data [45]. The predicted shape of the z dependence and the quadratic nuclear size dependence agrees well with the experimental data. The energy dependence of the suppression also has excellent agreement with our prediction. What is amazing is the clear quadratic $A^{2/3}$ nuclear size dependence of the suppression which is a true QCD non-Abelian effect. In fitting the data of the overall suppression for ^{14}N target we obtain the only parameter in our calculation, $\widetilde{C}\alpha_{\rm s}^2 = 0.00065\ \mathrm{GeV}^2$.

One can also calculate theoretically the average energy loss by the quark,

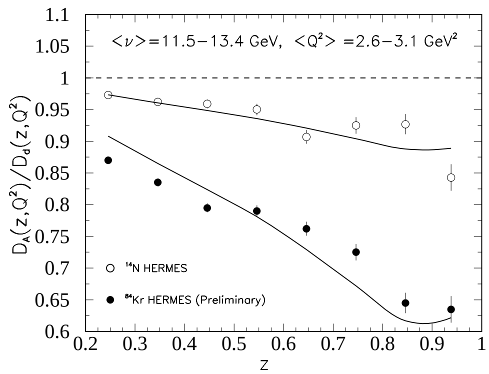

Figure 3. The predicted nuclear modification of jet fragmentation function is compared to the HERMES data [45].

which is the energy carried away by the radiated gluons,

$$\Delta E = \nu\langle \Delta z_g \rangle \approx \widetilde{C}(C_A \alpha_s^2/N_c) 3 \ln(1/2x_B). \tag{10}$$

With the value of $\alpha_s^2 \widetilde{C}$, one gets the quark energy loss $dE/dx \approx 0.3$ GeV/fm for the Kr target.

6 Jet quenching in heavy-ion collisions

In high-energy heavy-ion collisions, the jet production rate is not affected by the formation of dense matter and the final state multiple scattering. One can assume that the high p_T hadron spectra can then be given by the convolution of the jet production cross section and the medium modified jet fragmentation function $\widetilde{D}_{h/c}(z_c, Q^2)$.

In principle, one should use the modified fragmentation function evaluated according to the pQCD calculation for a dense medium. However, before that can be done in a practical manner, we have used the effective approach in Eq. (9) by rescaling the fractional momentum by $1 - \Delta z$ to take into account of the parton energy loss. To verify whether such an effective approach is adequate, we compare the two modified fragmentation functions in Fig. 4. We found that the effective model (dashed lines) can reproduce the pQCD result (solid lines) very well, but only when Δz is set to be $\Delta z \approx 0.6\langle z_g \rangle$. Therefore the actual averaged parton energy loss should be about 1.6 times of that used in the effective modified fragmentation function. This difference

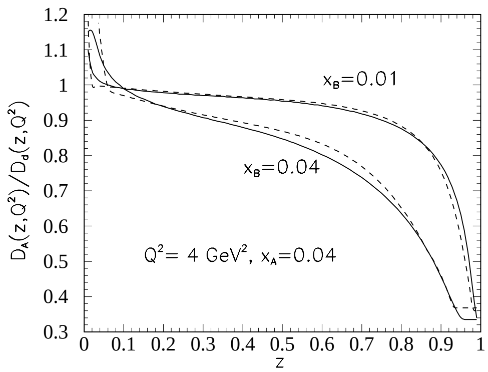

Figure 4. Comparison of the calculated nuclear modification with the effective model in Eq. (9) with $\Delta z = 0.6\langle z_g\rangle$.

is caused by the absorptive processes or unitarity correction effect in the full pQCD calculation.

Unlike in DIS nuclear scattering, the dense medium in high-energy heavy-ion collisions is not static. It has to go through rapid expansion which should also affect the effective total parton energy loss. The total energy loss extracted from experiments should be a quantity that is averaged over the whole evolution history of the expanding system. It is therefore useful to convert the averaged quantity to an energy loss in a static system that has the same parton density as the expanding system at its initial stage. If the averaged total parton energy loss in a longitudinally expanding system with a transverse size R is $\Delta E_{1\mathrm{d}}$, one finds [39] that the corresponding parton energy loss in a static system with the same initial parton density would be $\Delta E = \Delta E_{1\mathrm{d}}(R/2\tau_0)$. Here τ_0 is the initial formation time of the dense medium.

Comparing the recent PHENIX data [46] with pQCD parton model calculation as shown in Fig. 5, one can extract a value of dE/dx=0.25 GeV/fm that one needs to use in the effective modified fragmentation function in fitting the data. Taking into account the unitarity correction effect and the expansion, this corresponds to an effective energy loss $dE/dx = 1.6\times 0.25R/2\tau_0$ in a static system with a density similar to the initial stage of the expanding system at τ_0. With $R \sim 6$ fm and $\tau_0 \sim 1/p_0 = 0.2$ fm, this would give $dE/dx \approx 12$ GeV/fm, which is about 40 times of that in a cold nuclear matter as extracted from the DIS processes. Since the parton energy loss is directly proportional to gluon density, this implies that the gluon density in the initial stage of $Au + Au$ collisions is about 40 times higher than that inside a cold nucleus.

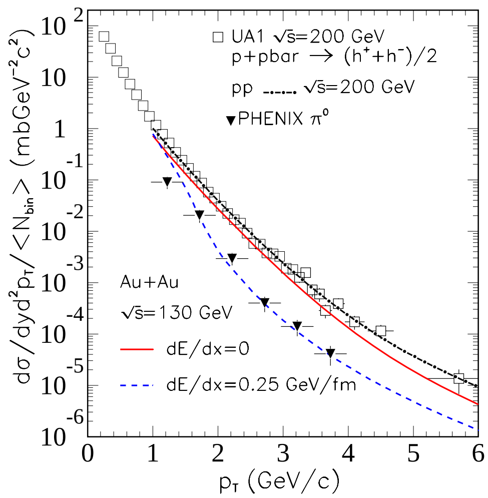

Figure 5. pQCD parton model calculation of the charged hadron and pion spectra in $p\bar{p}$ and central $Au + Au$ collisions compared with the experimental data [46,47]. The effective modified fragmentation function is used in the calculation.

7 Conclusions

Recent RHIC data require a strong shadowing of gluon distribution in nuclei within a two-component model of particle production in heavy-ion collisions. Using this strong gluon shadowing with an assumed impact-parameter dependence, the predicted centrality dependence of the hadron multiplicity agrees well with the recent RHIC results. The results are compared with the parton saturation model [15,16]. In order to differentiate the two models one needs more accurate experimental data in both the most central and peripheral regions of centrality or study the centrality dependence of the ratios at different colliding energies.

It is argued that the jet quenching will not contribute much to the total hadron multiplicity due to detailed balance in a thermal environment, even though they significantly suppress the high p_T spectra. The medium modification of the jet fragmentation functions due to gluon radiation induced by the multiple parton scattering can be calculated in pQCD. The predictions of the shape, energy dependence, and the quadratic nuclear size $A^{2/3}$ dependence of the modification agree well with the recent HERMES data. The resultant parton energy loss in the cold nuclear medium is estimated to be about 0.3

GeV/fm inside Kr nuclei. Comparing to the QCD result of the modification of fragmentation function, the actual averaged energy loss is found to be about 1.6 times that of the effective energy loss used in a earlier effective model for the same modification. Considering the effect of expansion, the recent PHENIX data imply a medium induced energy loss in central $Au + Au$ collisions equivalent to 12 GeV/fm in a static medium with the same gluon density as in the initial stage of the collision.

Acknowledgments

This work is supported by the Director, Office of Energy Research, Office of High Energy and Nuclear Physics, Division of Nuclear Physics, and by the Office of Basic Energy Science, Division of Nuclear Science, of the U.S. Department of Energy under Contract No. DE-AC03-76SF00098 and in part by NSFC under project 19928511 and 10075031.

References

1. T. K. Gaisser and F. Halzen, Phys. Rev. Lett. **54**, 1754 (1985).
2. G. Pancheri and Y. N. Srivastava, Phys. Lett. B **182**, 199 (1986).
3. W. R. Chen and R. C. Hwa, Phys. Rev. D **39**, 179 (1989).
4. X.-N. Wang, Phys. Rev. D **43**, 104 (1991).
5. J. P. Blaizot and A. H. Mueller, Nucl. Phys. **B289**, 847 (1987).
6. K. Kajantie, P. V. Landshoff and J. Lindfors, Phys. Rev. Lett. **59**, 2527 (1987); K. J. Eskola, K. Kajantie and J. Lindfors, Nucl. Phys. B **323**, 37 (1989).
7. X.-N. Wang and M. Gyulassy, Phys. Rev. D **44**, 3501 (1991); Comput. Phys. Commun. **83**, 307 (1994) [arXiv:nucl-th/9502021].
8. X.-N. Wang, Phys. Rept. **280**, 287 (1997) [arXiv:hep-ph/9605214].
9. X.-N. Wang and M. Gyulassy, Phys. Rev. Lett. **86**, 3496 (2001) [arXiv:nucl-th/0008014].
10. B. B. Back *et al.* [PHOBOS Collaboration], Phys. Rev. Lett. **85**, 3100 (2000) [arXiv:hep-ex/0007036]; arXiv:nucl-ex/0105011.
11. B. B. Back *et al.* [PHOBOS Collaboration], arXiv:nucl-ex/0108009.
12. K. Adcox *et al.* [PHENIX Collaboration], Phys. Rev. Lett. **86**, 3500 (2001) [arXiv:nucl-ex/0012008].
13. C. Adler *et al.* [STAR Collaboration], Phys. Rev. Lett. **87**, 112303 (2001) [arXiv:nucl-ex/0106004].
14. I. G. Bearden *et al.* [BRAHMS Collaborations], arXiv:nucl-ex/0108016.

15. D. Kharzeev and M. Nardi, Phys. Lett. B **507**, 121 (2001) [arXiv:nucl-th/0012025].
16. D. Kharzeev and E. Levin, arXiv:nucl-th/0108006.
17. M. Gluck, E. Reya and A. Vogt, Z. Phys. C **67**, 433 (1995).
18. UA5 Collaboration, G.J. Alner et al., Z. Phys. C**33**, 1 (1986).
19. Aachen-CERN-Heidelberg-Munich Collaboration, W. Thome et al., Nucl. Phys. **B129**, 365 (1977).
20. J. Whitmore, Phys. Rept. **10**, 273 (1974).
21. NA49 Collaboration, H. Appelshauser et al.,[NA49 Collaboration], Phys. Rev. Lett. **82** 2471 (1999) [arXiv:nucl-ex/9810014]; C. Hohne [NA49 Collaboration], Nucl. Phys. **A661** 485c (1999).
22. A. Bialas, M. Bleszynski and W. Czyz, Nucl. Phys. B **111**, 461 (1976).
23. S. Y. Li and X. N. Wang, arXiv:nucl-th/0110075.
24. K. J. Eskola, K. Kajantie, P. V. Ruuskanen and K. Tuominen, Nucl. Phys. B **570**, 379 (2000) [arXiv:hep-ph/9909456]; K. J. Eskola, K. Kajantie and K. Tuominen, arXiv:hep-ph/0106330.
25. A. Capella and D. Sousa, Phys. Lett. B **511**, 185 (2001) [arXiv:nucl-th/0101023]; N. Armesto, C. Pajares and D. Sousa, arXiv:hep-ph/0104269; J. Dias de Deus and R. Ugoccioni, Phys. Lett. B **494**, 53 (2000) [arXiv:hep-ph/0009288]; H. J. Pirner and F. Yuan, Phys. Lett. B **512**, 297 (2001) [arXiv:hep-ph/0101115]; B. H. Sa, A. Bonasera, A. Tai and D. M. Zhou, arXiv:nucl-th/0108003.
26. L. McLerran, R. Venugopalan Phys. Rev. **D49** 2233 (1994) [arXiv:hep-ph/9309289], A. Krasnitz, R. Venugopalan Phys. Rev. Lett. **84** 4309 (2000) [arXiv:hep-ph/9909203].
27. X.-N. Wang and M. Gyulassy, Phys. Rev. Lett. **68**, 1480 (1992).
28. E. Wang and X.-N. Wang, Phys. Rev. Lett. **87**, 142301 (2001) [arXiv:nucl-th/0106043].
29. J. D. Bjorken, Fermilab-Pub-82/59-THY (1982) and erratum (unpublished).
30. M. H. Thoma and M. Gyulassy, Nucl. Phys. B **351** (1991) 491.
31. S. J. Brodsky and P. Hoyer, Phys. Lett. B **298** (1993) 165 [arXiv:hep-ph/9210262].
32. L. D. Landau and I. J. Pomeranchuk, Dokl. Akad. Nauk Ser.Fiz. 92 (1953) 92; A. B. Migdal, Phys. Rev. **103** (1956) 1811.
33. M. Gyulassy and X.-N. Wang, Nucl. Phys. B **420** (1994) 583 [arXiv:nucl-th/9306003]; X.-N. Wang, M. Gyulassy and M. Plumer, Phys. Rev. D **51** (1995) 3436 [arXiv:hep-ph/9408344].
34. R. Baier, Y. L. Dokshitzer, S. Peigne and D. Schiff, Phys. Lett. B **345** (1995) 277 [arXiv:hep-ph/9411409]; R. Baier, Y. L. Dokshitzer,

A. H. Mueller, S. Peigne and D. Schiff, Nucl. Phys. B **484** (1997) 265 [arXiv:hep-ph/9608322].
35. B. G. Zakharov, JETP Lett. **63** (1996) 952 [arXiv:hep-ph/9607440].
36. M. Gyulassy, P. Levai and I. Vitev, Phys. Rev. Lett. **85** (2000) 5535 [arXiv:nucl-th/0005032]; M. Gyulassy, P. Levai and I. Vitev, Nucl. Phys. B **594** (2001) 371 [arXiv:nucl-th/0006010].
37. U. A. Wiedemann, Nucl. Phys. A **690** (2001) 731 [arXiv:hep-ph/0008241].
38. R. Baier, Y. L. Dokshitzer, A. H. Mueller and D. Schiff, Phys. Rev. C **58** (1998) 1706 [arXiv:hep-ph/9803473].
39. M. Gyulassy, I. Vitev and X.-N. Wang, Phys. Rev. Lett. **86** (2001) 2537 [arXiv:nucl-th/0012092]; M. Gyulassy, I. Vitev, X.-N. Wang and P. Huovinen, arXiv:nucl-th/0109063.
40. R. Baier, Y. L. Dokshitzer, A. H. Mueller and D. Schiff, Phys. Rev. C **60** (1999) 064902 [arXiv:hep-ph/9907267].
41. K. Adcox *et al.* [PHENIX Collaboration], Phys. Rev. Lett. **87** (2001) 052301 [arXiv:nucl-ex/0104015].
42. X.-N. Wang and M. Gyulassy, "Jets In Relativistic Heavy Ion Collisions", LBL-29390 *Presented at Workshop on Experiments and Detectors for RHIC, Upton, N.Y., Jul 2-7, 1990.*
43. X.-N. Wang, Z. Huang and I. Sarcevic, Phys. Rev. Lett. **77** (1996) 231 [arXiv:hep-ph/9605213]; X.-N. Wang and Z. Huang, Phys. Rev. C **55** (1997) 3047 [arXiv:hep-ph/9701227].
44. X. F. Guo and X.-N. Wang, Phys. Rev. Lett. **85** (2000) 3591 [arXiv:hep-ph/0005044]; X. N. Wang and X. F. Guo, arXiv:hep-ph/0102230.
45. V. Muccifora [HERMES Collaboration], arXiv:hep-ex/0106088.
46. K. Adcox *et al.* [PHENIX Collaboration], arXiv:nucl-ex/0109003.
47. C. Albajar *et al.* [UA1 Collaboration], Nucl. Phys. B **335** (1990) 261.